Journal Pre-proof

Nonbinary ldpc-coded probabilistic shaping scheme for MIMO systems based on signal space diversity

Weimin Kang

PII: S2352-8648(22)00085-2

DOI: https://doi.org/10.1016/j.dcan.2022.04.029

Reference: DCAN 418

To appear in: *Digital Communications and Networks*

Received Date: 2 August 2021

Revised Date: 28 April 2022

Accepted Date: 28 April 2022

Please cite this article as: W. Kang, Nonbinary ldpc-coded probabilistic shaping scheme for MIMO systems based on signal space diversity, *Digital Communications and Networks* (2022), doi: https://doi.org/10.1016/j.dcan.2022.04.029.

Digital Communications and Networks(DCN)

HOSTED BY

ELSEVIER

Available online at www.sciencedirect.com

ScienceDirect

journal homepage: www.elsevier.com/locate/dcan

Nonbinary ldpc-coded probabilistic shaping scheme for MIMO systems based on signal space diversity

Weimin Kang*

School of Information and Communication Engineering, North University of China, Taiyuan 030051, China

Abstract

This paper first describes a binary Low-Density Parity-Check (LDPC)-coded Probabilistic Shaping (PS) scheme for Multiple-Input Multiple-Output (MIMO) systems based on Signal Space Diversity (SSD). Second, a Nonbinary (NB) LDPC-coded PS scheme for MIMO systems based on SSD is proposed. The first scheme can be used to obtain a shaping gain, whereas the second can also realize a coding gain. The theoretical average mutual information of the optimized rotated quadrature amplitude modulation constellations is analyzed and the simulated error performance with 2×2 and 4×4 MIMO schemes is investigated. The theoretical average mutual information analysis and simulation results show that the proposed NB LDPC-coded PS scheme for MIMO systems based on SSD is reliable and robust, and is therefore suitable for future wireless communication systems.

KEYWORDS: Probabilistic shaping, Multiple-input multiple-output, Signal space diversity, Average mutual information.

1. Introduction

To satisfy the growing demand for data traffic, future communication systems require ultra-energy-efficient transmission and high Spectral Efficiency (SE) [1–5]. Multiple-Input Multiple-Output (MIMO) systems use multiple transmitter antennas and multiple receiver antennas for data transmission, enabling spatial multiplexing gain and spatial diversity gain, i.e., improved transmission rates and reliability [6]. Precoding and space-time coding [7] are effective methods for improving the error performance of fading channels. Precoding based on Singular Value Decomposition (SVD) requires complete Channel State Information (CSI) at both the transmitter and receiver [8]. After passing through the SVD channel matrix, the receiver has L independent Single-Input Single-Output (SISO) channels, where L denotes the number of transmitted layers. To obtain a diversity gain and improve error performance in fading channels, Signal Space Diversity (SSD) [9] can be obtained through a combination of optimized rotated constellations and component interleaving. The application of SSD in MIMO systems has been investigated in [10, 11]. In [12], a precoded MIMO scheme with SSD was developed to improve the reliability of the system.

In most conventional MIMO systems, regular uniform Quadrature Amplitude Modulation (QAM) constellations are used, although this can result in shaping loss compared with Gaussian-distributed input data [13]. To obtain a shaping gain, Geometric Shaping (GS) [14–16] and Probabilistic Shaping (PS) [17–19] can be used. The constellation points of GS are nonuniformly distributed with equal probability, whereas the constellation points of PS are equally spaced with unequal probability. The optimization of GS constellations is based on the Signal-to-Noise Ratio (SNR) and SE. A constant composition distribution matcher [20] is used to generate an unequal amplitude distribution in the PS scheme. Most previous work on PS [21–24] has assumed an additive

*Corresponding author (email: kwm2013@126.com).

white Gaussian noise channel. For Rayleigh fading channels, a rotated-QAM-based PS scheme for SISO systems has been investigated [25], and this achieved higher SE than conventional regular uniform QAM systems. PS has more significant advantage than GS, is sufficiently flexible for rate adaptation, and enables simpler hardware implementation.

For Fifth-Generation (5G) mobile communication, Low-Density Parity-Check (LDPC) codes are used in the uplink and downlink encoding schemes of data channels [26, 27]. Compared with binary LDPC codes, the parity check matrix of Nonbinary (NB) LDPC codes over the Galois field GF(q) is sparser [28, 29], making NB LDPC codes more suitable for high-order modulation systems [30, 31]. The combination of NB LDPC codes and MIMO transmission was proposed in [32]. Compared with binary LDPC codes, the combination of NB LDPC codes and MIMO transmission realizes a coding gain that can significantly improve the error performance of the system.

In this paper, we first propose a binary LDPC-coded PS scheme for MIMO systems based on SSD. Second, to obtain a coding gain, an NB LDPC-coded PS scheme for MIMO systems based on SSD is proposed. Compared with conventional binary LDPC-coded regular QAM MIMO systems in fading channels, the combination of NB LDPC-coded PS and SSD in MIMO systems achieves a coding gain, shaping gain, and diversity gain. The theoretical Average Mutual Information (AMI) and simulation results show that the proposed NB LDPC-coded PS scheme for MIMO systems based on SSD is reliable and robust, and is therefore suitable for Sixth-Generation (6G) communication systems.

Throughout this paper, $E[\cdot]$ denotes the expectation, $(\cdot)^T$ represents transposition, $(\cdot)^H$ denotes conjugate transposition, and $(\cdot)_I$, $(\cdot)_Q$ denote in-phase and quadrature components, respectively.

The remainder of this paper is organized as follows. In Section 2, the system model of the proposed NB LDPC-coded PS scheme for MIMO systems based on SSD is proposed. AMI analysis of the proposed scheme in fast fading channels is discussed in Section 3. Simulation results are presented in Section 4. Finally, Section 5 gives the conclusions to this study.

2. System model

The system model of the proposed NB LDPC-coded PS scheme for MIMO systems based on SSD is shown in Fig. 1. Assume that perfect CSI is known for both the transmitter and the receiver. In Fig. 1, the $N_R \times N_T$ MIMO system has rank L, where N_R and N_T denote the number of receiver and transmitter antennas, respectively. In the transmitters, k uniformly distributed data bits U_{bin}^A pass through the Distribution Matcher (DM) according to the probability distribution P_A, and are then assigned n nonuniformly distributed amplitudes A. The DM suffers some code rate loss. The code rate of the DM is

$$r_{dm} = k/n \tag{1}$$

As $n \to \infty$,

$$\lim_{n\to\infty} \frac{k}{n} = H(P_A) \tag{2}$$

where $H(P_A)$ denotes the entropy of the unequal amplitude probability distribution P_A. The length of k is $\left\lfloor \log_2 \left| T_{P_A}^n \right| \right\rfloor$, where $T_{P_A}^n$ denotes a set of vectors of length n satisfying probability distribution P_A, and $\lfloor \cdot \rfloor$ represents the rounding down operation. One gray-labeled M-QAM symbol consists of two orthogonal $\sqrt{M}$ Pulse Amplitude Modulation (PAM) symbols, i.e., for 16QAM symbols and 64QAM symbols, the one-dimensional 4PAM and 8PAM schemes can be considered, respectively. The amplitude set $A = \{3.0, 1.0\}$ is used for the 4PAM constellation symbols, while the amplitude set $A = \{7.0, 5.0, 3.0, 1.0\}$ is considered for the 8PAM constellation symbols.

The amplitude labeling function $\chi_A(\cdot)$ maps symbols to a binary bit sequence. For the 4PAM symbols,

$$\chi_A(3) = 1 \quad \chi_A(1) = 0 \tag{3}$$

and for the 8PAM symbols,

$$\chi_A(7) = 00 \quad \chi_A(5) = 01 \quad \chi_A(3) = 11 \quad \chi_A(1) = 10 \tag{4}$$

The labeled nonuniformly distributed data bits b_{bin} are used for the amplitude part of the modulation symbols. Assume that the LDPC code rate is r and the uniform data bits U_{bin}^S have a length of γ_n, with

$$\gamma_n = mnr - (m-1)n \tag{5}$$

where $m = \log_2 M/2$. $\gamma_n \geq 0$ means that the LDPC code rate must be no less than $(m-1)/m$. The total code rate R can be computed as follows:

$$R = \frac{k+\gamma_n}{mn} = \frac{k+mnr-(m-1)n}{mn} = \frac{1}{m}\cdot\frac{k}{n} + r - \frac{m-1}{m} \tag{6}$$

The data bits b_{bin} and U_{bin}^S are converted into input information symbols for the NB LDPC code by Series-to-Parallel (S/P) conversion, which generates u^A and u^S, respectively. The generated parity symbols c are then converted into data bits g by Parallel-to-Series (P/S) conversion. The connection of data bits U_{bin}^S and g is used for the sign part of the modulation symbols. To achieve a diversity gain on fading channels, the modulated symbols $s = \{s_I, s_Q\}^T$ are then rotated and the symbols $x = \{x_I, x_Q\}^T$ are generated. These symbols can be expressed as follows:

$$\begin{bmatrix} x_I \\ x_Q \end{bmatrix} = \begin{bmatrix} \cos\theta & \sin\theta \\ -\sin\theta & \cos\theta \end{bmatrix} \begin{bmatrix} s_I \\ s_Q \end{bmatrix} \tag{7}$$

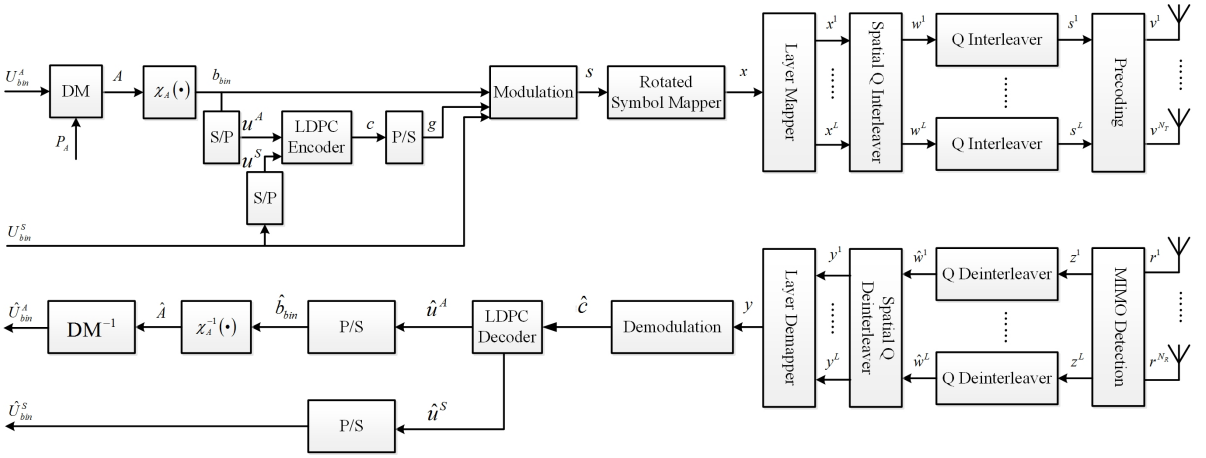

Fig. 1: System model of proposed NB LDPC-coded PS scheme for MIMO systems based on SSD.

where θ denotes the angle of rotation. The rotated symbols x are then mapped to L layers, and a spatial Q-component interleaver is applied to the Q components of the symbols in L layers. The Q-component interleaver has no effect on the I-component of the symbol. Therefore, the I-component of the symbol and the Q-component of the symbol after the spatial Q-component interleaver are subjected to different fading rates, which reduces the correlation between the spatial I-component and Q-component. To reduce the correlation between the I-component and Q-component in the time domain, the Q-interleaver is applied to all layers, which are interleaved by a pseudo S-random interleaver. The symbols are then subjected to spatial precoding and mapped to the N_T transmitter antennas.

We obtain the spatial precoding matrix using SVD, and decompose the $N_R \times N_T$ MIMO channel matrix H as

$$H = U\Lambda V^H \tag{8}$$

where U and V are $N_R \times N_R$ and $N_T \times N_T$ matrices, respectively. U and V are unitary matrices. Λ is an $N_R \times N_T$ diagonal matrix with rank L. V is the precoding matrix and U^H is the MIMO detection matrix. Thus, after MIMO detection, the symbols z can be expressed as

$$z = U^H HVs + U^H n = \Lambda s + n' \tag{9}$$

where n and n' denote the column vectors of $N_R \times 1$ complex Gaussian random variables with means of zero and variances of $\sigma^2 = \frac{N_0}{2}$. Here, N_0 denotes the single power spectral density. After passing through the time-domain Q-deinterleaver and the spatial Q-deinterleaver, the received symbols y are generated for the L layers: $y = [y_1, \cdots, y_L]^T$. y_i is demodulated by calculating $l_{i,j}$:

$$l_{i,j} = \ln \frac{P_{B_j}(0)}{P_{B_j}(1)} + \ln \frac{q_{i,j}(y_i|0)}{q_{i,j}(y_i|1)} \tag{10}$$

$$P_{B_j}(b) = \sum_{a\in\{0,1\}^f : a_j = b} P_B(a) \tag{11}$$

where $P_{B_j}(b)$ denotes the probability that the j-th bit-level of symbol B is b, $b \in \{0, 1\}$. $B = B_1B_2 \cdots B_m = label(x_i), i = 1, 2, \cdots, n$, where $label(\cdot)$ represents symbol-to-bit mapping.

$$q_{i,j}(y|b) = \sum_{a\in\{0,1\}^f : a_j = b} q_c(y_i|x_a) \frac{P_B(a)}{P_{B_j}(b)} \tag{12}$$

where $i = 1, 2, \cdots, n$, $j = 1, 2, \cdots, f$, $f = \log_2 M$, and $q_c(\cdot|\cdot)$ denotes the conditional probability density function. The rotated constellation is $x_a = \{x_{a_I}, x_{a_Q}\}$, where x_{a_I} and x_{a_Q} represent the real and imaginary parts of x_a, respectively.

$$q_c(y|x_a) = \frac{1}{\sqrt{2\pi\sigma^2}} \exp \frac{-(y_I - |h_I| \cdot x_{a_I})^2 - (y_Q - |h_Q| \cdot x_{a_Q})^2}{2\sigma^2} \tag{13}$$

where h_I and h_Q denote the real and imaginary parts of fading channels, respectively.

The demodulated bit probability satisfies

$$P(y_{i,j} = 0) + P(y_{i,j} = 1) = 1 \tag{14}$$

$$l_{i,j} = \ln\left(\frac{P\left(y_{i,j} = 0\right)}{P\left(y_{i,j} = 1\right)}\right) \tag{15}$$

for $i = 1, 2 \cdots n$, $j = 1, 2, \cdots f$. The demodulated bit probability can then be written as

$$\begin{aligned} P(y_{i,j} = 0) &= \frac{1}{1 + \exp(-l_{i,j})} \\ P(y_{i,j} = 1) &= \frac{\exp(-l_{i,j})}{1 + \exp(-l_{i,j})} \end{aligned} \tag{16}$$

for $i = 1, 2 \cdots n$, $j = 1, 2, \cdots f$. After passing through the demodulator, the input to the GF(q) LDPC decoder can be calculated as

$$P_i(c) = \frac{\tilde{P}_i(c)}{\sum_{c'\in GF(q)} \tilde{P}_i(c')} = \frac{\prod_{j=1}^{p} \tilde{P}_{i,j}}{\sum_{c'\in GF(q)} \tilde{P}_i(c')} \tag{17}$$

for $i = 1, 2 \cdots n$, $j = 1, 2, \cdots p$, $p = \log_2 q$, where

$$\tilde{P}_{i,j} = \begin{cases} P(y_{i,j} = 0) & if [\phi^{-1}_{GF(q)}(c)]_j = 0 \\ P(y_{i,j} = 1) & if [\phi^{-1}_{GF(q)}(c)]_j = 1 \end{cases} \quad (18)$$

in which $[\phi^{-1}_{GF(q)}(c)]_j$ is the j-th binary mapping bit of c for $c \in$GF(q).

The LDPC-decoded symbols $\hat{u}^A$ and $\hat{u}^S$ are then mapped into data bits $\hat{b}_{bin}$ and $\hat{U}^S_{bin}$, respectively, by P/S conversion. The amplitude inverse labeling function $\chi^{-1}_A(\cdot)$ and inverse DM are then applied, and the estimated transmitted bits $\{\hat{U}^A_{bin}, \hat{U}^S_{bin}\}$ are finally obtained.

3. AMI analysis

The AMI reflects the maximum information rate that can reliably be transmitted for a given system [33]. In this paper, we consider the Bit-Interleaved Coded Modulation (BICM) AMI in MIMO systems for fading channels. For M-ary QAM constellations, two orthogonal $\sqrt{M}$-PAM constellations are considered. The amplitude probability distribution is satisfied by the Maxwell–Boltzmann (M-B) distribution [34] for PS MIMO systems.

3.1. Optimal rotation angle based on AMI analysis

The BICM AMI for PS MIMO systems in fading channels is calculated as follows:

$$\begin{aligned} I_{BICM} &= \sum_{k=1}^{L} I(c_i, y|h) \\ &= L \cdot (-\sum_{i=1}^{M} P(x_i) \log_2 P(x_i)) \\ &\quad - L \cdot \sum_{i=1}^{\log_2 M} E_{c_i,y,h} \left[\log_2 \frac{\sum_{\bar{x} \in \chi} P(y|\bar{x}, h) P(\bar{x})}{\sum_{x \in \chi_{c_i}} P(y|x, h) P(x)} \right] \end{aligned} \quad (19)$$

where x and y denote the discrete input constellation point and the continuous output signal, respectively. χ and χ_{c_i} denote the constellation set and the constellation subset, respectively, where the i-th bit $c_i \in \{0, 1\}$. h represents the fading channel coefficients.

Using the AMI optimization criterion, for a given SNR, the optimal rotation angle θ^{opt} and $I_{BICM}(SNR, \theta^{opt})$ can be obtained. For a MIMO system with $N_R = N_T = 2, L = 2$, the curves of θ^{opt} versus $I_{BICM}(SNR, \theta^{opt})$ in PS 16QAM and PS 64QAM are shown in Figs. 2 and 3, respectively. For a MIMO system with $N_R = N_T = 4, L = 4$, the curves of θ^{opt} versus $I_{BICM}(SNR, \theta^{opt})$ in PS 16QAM and PS 64QAM are shown in Figs. 4 and 5, respectively. For the proposed L-layer MIMO system with a total code rate of R in M-QAM modulation, the theoretical maximum information rate is $I_{max} = LR \log_2 M$. As shown in Fig. 2 of [9], varying the rotation angle from 0–45 degrees is sufficient for constellation rotation optimization. Therefore, rotation angles of 0–45 degrees are considered in this paper.

In Fig. 2, for the 2 × 2 MIMO case, PS1 and PS2 for 4PAM are [3:1]=[0.3505:0.6495] and [3:1]=[0.333:0.667], respectively. The total code rates considered here are 4/5 and 5/6 for PS1 and PS2, respectively. The optimal rotation angles are 18 degrees for PS1, PS2, and the uniform 16QAM system in fast fading channels. In Fig. 3, the 2 × 2 MIMO scheme with 8PAM has PS3 and PS4 of [7:5:3:1]=[0.1265:0.213:0.30175:0.35875] and [7:5:3:1]=[0.1135:0.206: 0.3065:0.374], respectively. The total code rates considered here are 4/5 and 5/6 for PS3 and PS4, respectively. The optimal rotation angles are 14 degrees for PS3, PS4, and the uniform 64QAM system in fast fading channels. In Fig. 4, for the 4 × 4 MIMO system, the optimal rotation angles are 18 degrees for PS1, PS2, and the uniform 16QAM system in fast fading channels. Finally, in Fig. 5, the 4 × 4 MIMO scheme has optimal rotation angles of 14 degrees for PS3, PS4, and the uniform 64QAM system in fast fading channels. In summary, by traversing the search domain, we found that probabilistic shaping can be directly used in MIMO systems based on SSD. The optimal rotation angle of the proposed PS QAM MIMO system is the same as that of the conventional regular QAM MIMO system.

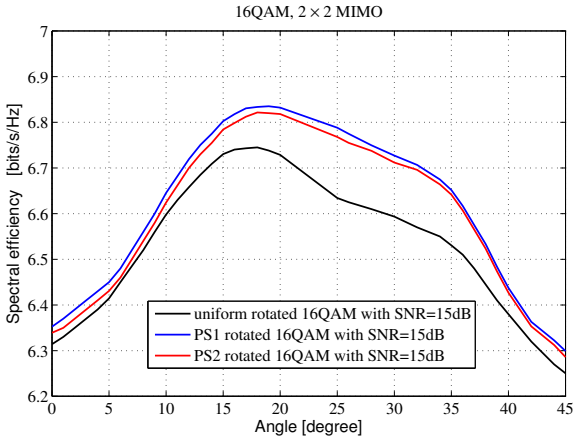

Fig. 2: SE vs. θ for 16QAM 2 × 2 MIMO at SNR=15 dB.

3.2. AMI analysis of the proposed scheme

In Figs. 6 and 7, the theoretical SE is analyzed for uniform 16QAM, uniform rotated 16QAM, and PS rotated 16QAM in 2×2 MIMO systems. In Fig. 6, when the SE is 6.4 bits/s/Hz, we achieve a diversity gain of 1.54 dB and a shaping gain of 0.40 dB using the PS1 16QAM 2 × 2 MIMO system with rotation of 18 degrees compared with the uniform 16QAM 2×2 MIMO system. In Fig. 7, when the SE is 6.667 bits/s/Hz, diversity and shaping gains of 2.00 dB and 0.30 dB,

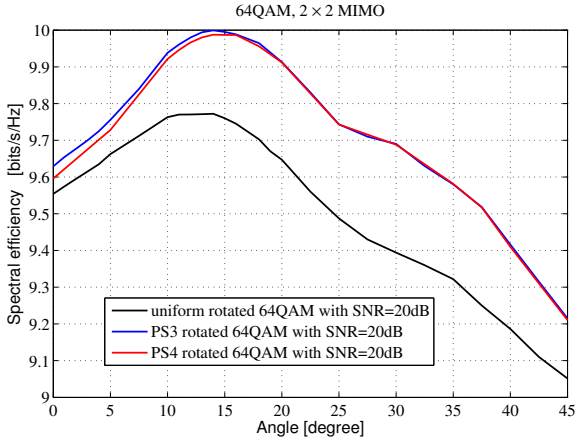

Fig. 3: SE vs. θ for 64QAM 2×2 MIMO at SNR=20 dB.

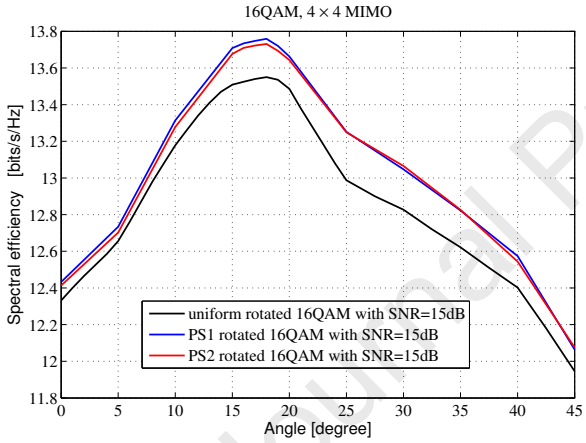

Fig. 4: SE vs. θ for 16QAM 4×4 MIMO at SNR=15 dB.

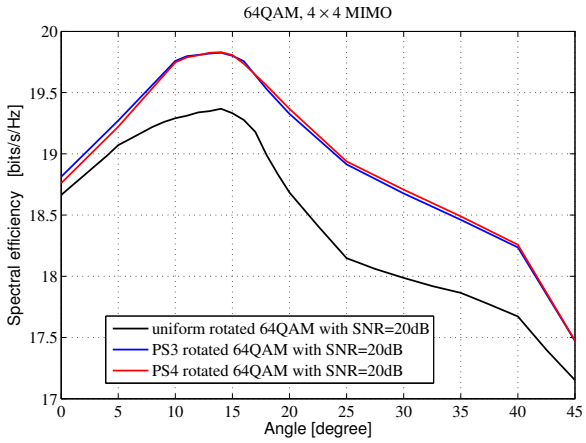

Fig. 5: SE vs. θ for 64QAM 4×4 MIMO at SNR=20 dB.

respectively, are realized with the PS2 16QAM 2×2 MIMO system with rotation of 18 degrees compared with the uniform 16QAM 2×2 MIMO system.

Figures 8 and 9 show the theoretical SE for uniform 64QAM, uniform rotated 64QAM, and PS rotated 64QAM in 2×2 MIMO systems. In Fig. 8, when the SE is 9.6 bits/s/Hz, we obtain a 0.65-dB diversity gain and 0.60-dB shaping gain using the PS3 64QAM 2×2 MIMO system with rotation of 14 degrees compared with the uniform 64QAM 2×2 MIMO system. In Fig. 9, when the SE is 10.0 bits/s/Hz, the diversity gain is 1.00 dB and the shaping gain is 0.50 dB using the PS4 64QAM 2×2 MIMO system with rotation of 14 degrees compared with the uniform 64QAM 2×2 MIMO system.

Figures 10 and 11 present the theoretical SE for uniform 16QAM, uniform rotated 16QAM, and PS rotated 16QAM in 4×4 MIMO systems. When the SE is 12.8 bits/s/Hz, Fig. 10 shows that there is a 2.23-dB diversity gain and 0.48-dB shaping gain using the PS1 16QAM 4×4 MIMO system with rotation of 18 degrees compared with the uniform 16QAM 4×4 MIMO system. In Fig. 11, when the SE is 13.334 bits/s/Hz, we find a 2.95-dB diversity gain and 0.31-dB shaping gain using the PS2 16QAM 4×4 MIMO system with rotation of 18 degrees compared with the uniform 16QAM 4×4 MIMO system.

Figures 12 and 13 illustrate the theoretical SE for uniform 64QAM, uniform rotated 64QAM, and PS rotated 64QAM in 4×4 MIMO systems. In Fig. 12, when the SE is 19.2 bits/s/Hz, we have a 1.08-dB diversity gain and 0.65-dB shaping gain using the PS3 64QAM 4×4 MIMO system with rotation of 14 degrees compared with the uniform 64QAM 4×4 MIMO system. In Fig. 13, when the SE is 20.0 bits/s/Hz, there is a 1.65-dB diversity gain and 0.55-dB shaping gain using the PS4 64QAM 4×4 MIMO system with rotation of 14 degrees compared with the uniform 64QAM 4×4 MIMO system.

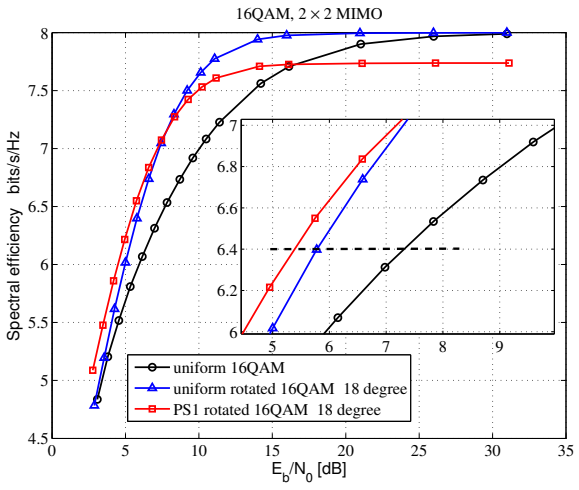

Fig. 6: 16QAM 2×2 MIMO AMI: comparison 1.

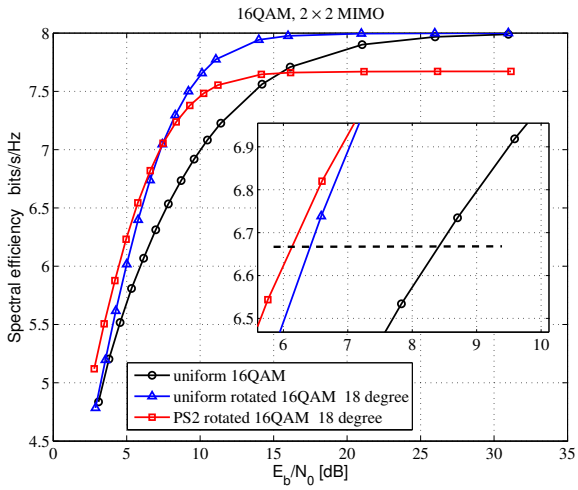

Fig. 7: 16QAM 2 × 2 MIMO AMI: comparison 2.

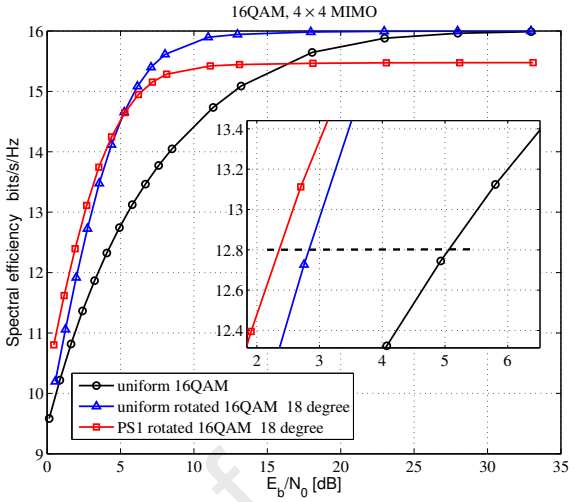

Fig. 10: 16QAM 4 × 4 MIMO AMI: comparison 1.

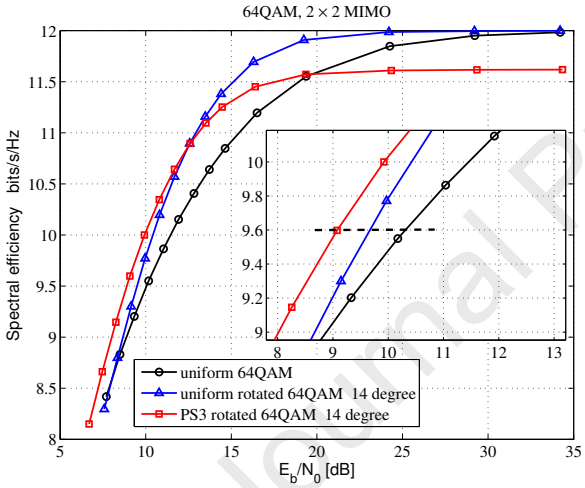

Fig. 8: 64QAM 2 × 2 MIMO AMI: comparison 1.

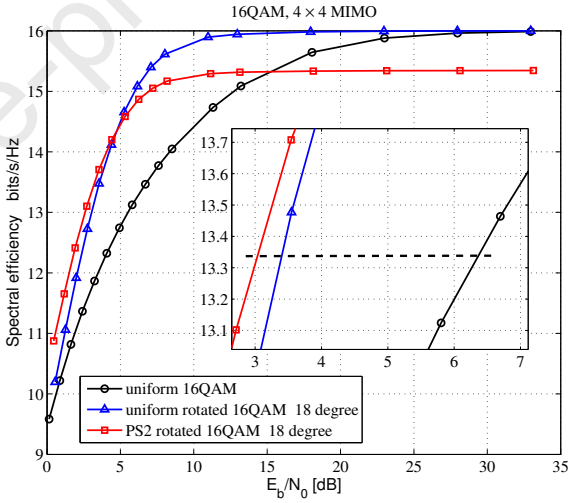

Fig. 11: 16QAM 4 × 4 MIMO AMI: comparison 2.

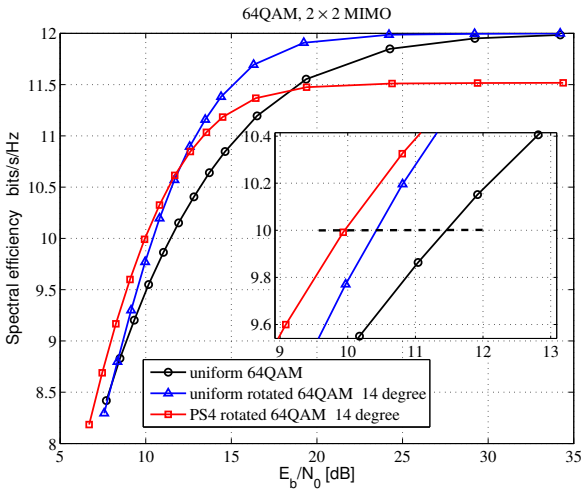

Fig. 9: 64QAM 2 × 2 MIMO AMI: comparison 2.

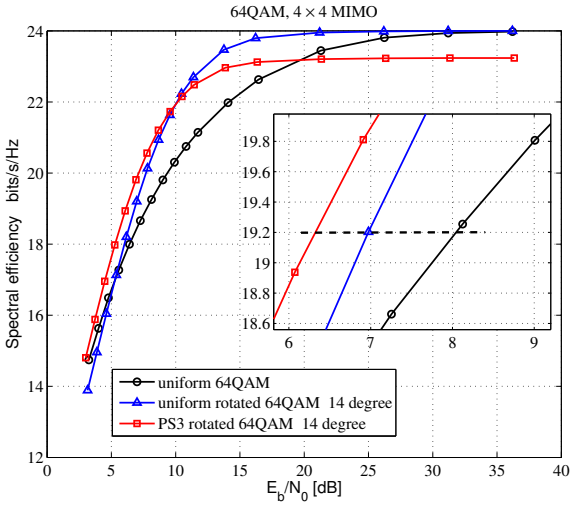

Fig. 12: 64QAM 4 × 4 MIMO AMI: comparison 1.

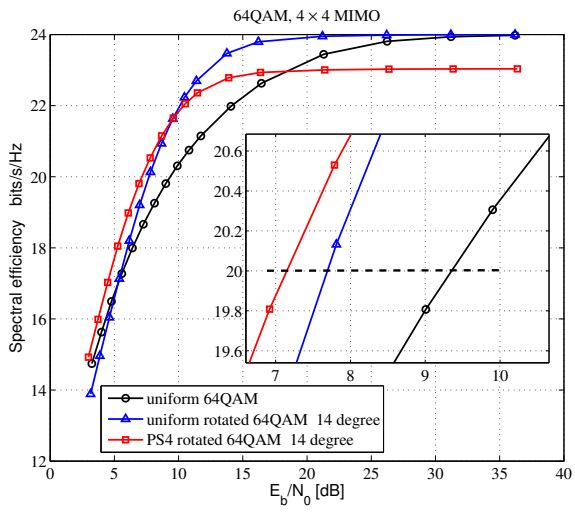

Fig. 13: 64QAM 4 × 4 MIMO AMI: comparison 2.

4. Simulation results

To evaluate the proposed NB LDPC-coded PS scheme for MIMO systems based on SSD in fast fading channels, Monte-Carlo simulations were conducted to verify the performance gain. The end-to-end Frame Error Rate (FER) performance was considered at 10^{-3}. The length codes of the binary LDPC were 12000 bits and 12600 bits with a constant variable node degree of $d_v = 3$ for 16QAM and 64QAM, respectively. To ensure a fair comparison, the code symbol lengths of the GF(16) LDPC and GF(64) LDPC were set to 3000 symbols and 2100 symbols, respectively. The average variable node degree of GF(16) LDPC codes is $d_v = 2.4$, whereas that of GF(64) LDPC codes is $d_v = 2$. The binary LDPC codes used the Log-BP decoding algorithm, whereas the NB LDPC codes used Log-FFT-BP decoding. The maximum decoding iteration time for both binary LDPC codes and NB LDPC codes was set to 30. The PS amplitude probability distribution satisfied the M-B distribution.

Figures 14 and 15 demonstrate the FER performance of the 16QAM 2 × 2 MIMO systems with SE of 6.4 bits/s/Hz and 6.667 bits/s/Hz, respectively. In Fig. 14, compared with the binary LDPC-coded uniform 16QAM no-rotation system with a code rate of 4/5, the optimized 18-degree rotation for the binary LDPC-coded uniform rotated 16QAM system obtains a 1.97-dB diversity gain, and a further 0.33-dB shaping gain can be achieved with the optimized 18-degree rotation in the binary LDPC-coded PS1 rotated 16QAM system. Thus, the total performance gain of the proposed binary LDPC-coded PS1 16QAM MIMO system with SSD is 2.30 dB. Compared with the binary LDPC-coded uniform 16QAM no-rotation system with a code rate of 4/5, the GF(16) LDPC-coded uniform 16QAM no-rotation system with a code rate of 4/5 obtains a 0.44-dB coding gain, and optimized 18-degree rotation for the GF(16) LDPC-coded uniform rotated 16QAM system gives a 1.88-dB diversity gain. A further 0.44-dB shaping gain can be produced using the optimized 18-degree rotation in the GF(16) LDPC-coded PS1 rotated 16QAM system. Compared with the GF(16) LDPC-coded uniform 16QAM no-rotation system with a code rate of 4/5, the total performance gain of the optimal GF(16) LDPC-coded PS1 rotated 16QAM system is 2.32 dB.

In Fig. 15, optimized 18-degree rotation for the binary LDPC-coded uniform rotated 16QAM system gives a 2.70-dB diversity gain compared with the binary LDPC-coded uniform 16QAM no-rotation system with a code rate of 5/6, and we can achieve a further 0.20-dB shaping gain with the optimized 18-degree rotation of the binary LDPC-coded PS2 rotated 16QAM system. Thus, the total performance gain of the proposed binary LDPC-coded PS2 16QAM MIMO system with SSD is 2.90 dB. Compared with the binary LDPC-coded uniform 16QAM no-rotation system with a code rate of 5/6, the GF(16) LDPC-coded uniform 16QAM no-rotation system with a code rate of 5/6 gives a 0.48-dB coding gain, and the optimized 18-degree rotation for the GF(16) LDPC-coded uniform rotated 16QAM system produces a 2.49-dB diversity gain. We get a further 0.30-dB shaping gain using the optimized 18-degree rotation in the GF(16) LDPC-coded PS2 rotated 16QAM system. Compared with the GF(16) LDPC-coded uniform 16QAM no-rotation system with a code rate of 5/6, the total performance gain of the optimal GF(16) LDPC-coded PS2 rotated 16QAM system is 2.79 dB.

Figures 16 and 17 show the FER performance of the 64QAM 2 × 2 MIMO systems with SE at 9.6 bits/s/Hz and 10.0 bits/s/Hz, respectively. In Fig. 16, compared with the binary LDPC-coded uniform 64QAM no-rotation system with a code rate of 4/5, the optimized 14-degree rotation for the binary LDPC-coded uniform rotated 64QAM system can obtain a 1.10-dB diversity gain. A further 0.50-dB shaping gain is achieved with the optimized 14-degree rotation in the binary LDPC-coded PS3 rotated 64QAM system, and so the total performance gain of the proposed binary LDPC-coded PS3 64QAM MIMO system with SSD is 1.60 dB. Compared with the binary LDPC-coded uniform 64QAM no-rotation system with a code rate of 4/5, the GF(64) LDPC-coded uniform 64QAM no-rotation system with a code rate of 4/5 exhibits a 0.70-dB coding gain. The optimized 14-degree rotation for the GF(64) LDPC-coded uniform rotated 64QAM system obtains 0.89-dB diversity gain, with a further 0.62-dB shaping gain for the optimized 14-degree rotation in the GF(64) LDPC-coded PS3 rotated 64QAM system. Compared with the GF(64) LDPC-coded uniform 64QAM no-rotation system with a code rate of 4/5, the total performance gain of the optimal GF(64) LDPC-coded PS3 rotated 64QAM system is 1.51 dB.

In Fig. 17, compared with the binary LDPC-coded

uniform 64QAM no-rotation system with a code rate of 5/6, the optimized 14-degree rotation for the binary LDPC-coded uniform rotated 64QAM system obtains a 1.50-dB diversity gain, with a further 0.32-dB shaping gain using the optimized 14-degree rotation in the binary LDPC-coded PS4 rotated 64QAM system. The total performance gain of the proposed binary LDPC-coded PS4 64QAM MIMO system with SSD is 1.82 dB. Compared with the binary LDPC-coded uniform 64QAM no-rotation system with a code rate of 5/6, the GF(64) LDPC-coded uniform 64QAM no-rotation system with a code rate of 5/6 obtains a 0.68-dB coding gain, whereas the optimized 14-degree rotation for the GF(64) LDPC-coded uniform rotated 64QAM system produces a 1.27-dB diversity gain. A further 0.40-dB shaping gain is given by the optimized 14-degree rotation in the GF(64) LDPC-coded PS4 rotated 64QAM system. Compared with the GF(64) LDPC-coded uniform 64QAM no-rotation system with a code rate of 5/6, the total performance gain of the optimal GF(64) LDPC-coded PS4 rotated 64QAM system is 1.67 dB.

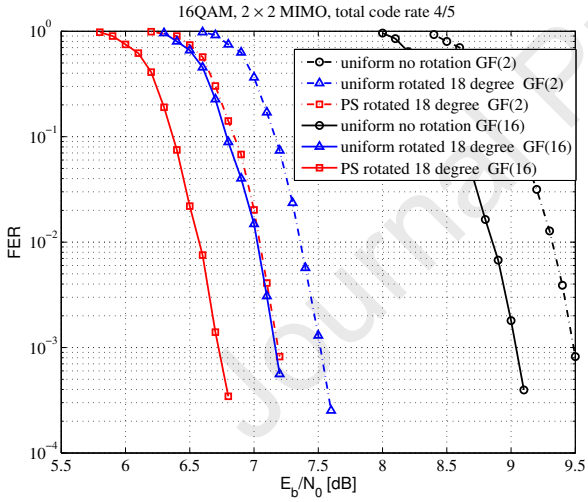

Fig. 14: FER performance of 16QAM 2 × 2 MIMO systems with SE at 6.4 bits/s/Hz.

Figures 18 and 19 demonstrate the FER performance of the 16QAM 4 × 4 MIMO systems with SE at 12.8 bits/s/Hz and 13.334 bits/s/Hz, respectively. In Fig. 18, compared with the binary LDPC-coded uniform 16QAM no-rotation system with a code rate of 4/5, the optimized 18-degree rotation in the binary LDPC-coded uniform rotated 16QAM system obtains a 3.00-dB diversity gain, with a further 0.49-dB shaping gain using the optimized 18-degree rotation in the binary LDPC-coded PS1 rotated 16QAM system. The total performance gain of the proposed binary LDPC-coded PS1 16QAM MIMO system with SSD is 3.49 dB. Compared with the binary LDPC-coded uniform 16QAM no-rotation system with a code rate of 4/5, the GF(16) LDPC-coded uniform 16QAM no-

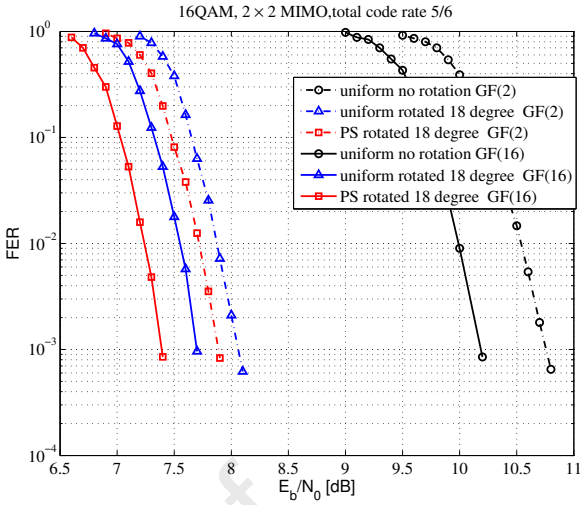

Fig. 15: FER performance of 16QAM 2 × 2 MIMO systems with SE at 6.667 bits/s/Hz.

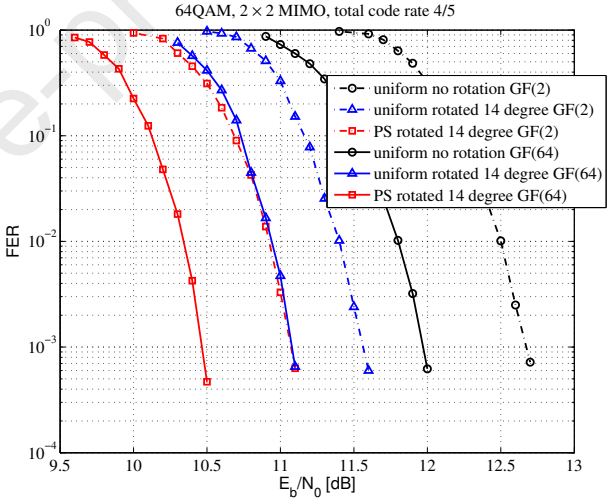

Fig. 16: FER performance of 64QAM 2 × 2 MIMO systems with SE at 9.6 bits/s/Hz.

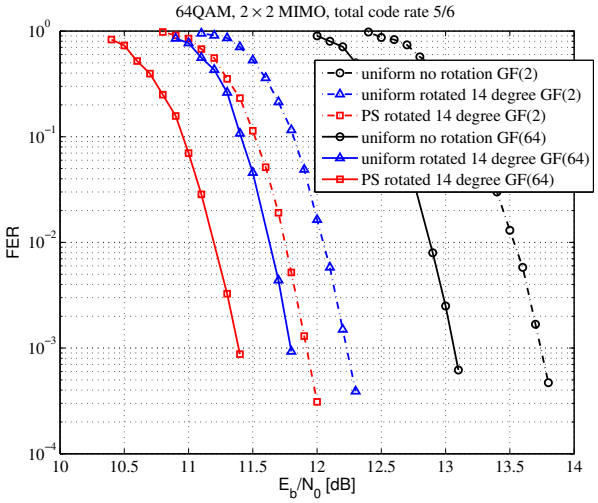

Fig. 17: FER performance of 64QAM 2 × 2 MIMO systems with SE at 10.0 bits/s/Hz.

rotation system with a code rate of 4/5 can obtain a 0.53-dB coding gain, whereas the optimized 18-degree rotation of the GF(16) LDPC-coded uniform rotated 16QAM system produces a 2.76-dB diversity gain. A further 0.61-dB shaping gain is achieved by the optimized 18-degree rotation in the GF(16) LDPC-coded PS1 rotated 16QAM system. Compared with the GF(16) LDPC-coded uniform 16QAM no-rotation system with a code rate of 4/5, the total performance gain of the optimal GF(16) LDPC-coded PS1 rotated 16QAM system is 3.37 dB.

In Fig. 19, compared with the binary LDPC-coded uniform 16QAM no-rotation system with a code rate of 5/6, the optimized 18-degree rotation of the binary LDPC-coded uniform rotated 16QAM system gives a 3.75-dB diversity gain, and a further 0.30-dB shaping gain is achieved by the optimized 18-degree rotation in the binary LDPC-coded PS2 rotated 16QAM system. Thus, the total performance gain of the proposed binary LDPC-coded PS2 16QAM MIMO system with SSD is 4.05 dB. Compared with the binary LDPC-coded uniform 16QAM no-rotation system with a code rate of 5/6, the GF(16) LDPC-coded uniform 16QAM no-rotation system with a code rate of 5/6 exhibits a 0.40-dB coding gain, and the optimized 18-degree rotation of the GF(16) LDPC-coded uniform rotated 16QAM system gives a 3.65-dB diversity gain. A further 0.47-dB shaping gain is produced by the optimized 18-degree rotation of in GF(16) LDPC-coded PS2 rotated 16QAM system. Compared with the GF(16) LDPC-coded uniform 16QAM no-rotation system with a code rate of 5/6, the total performance gain of the optimal GF(16) LDPC-coded PS2 rotated 16QAM system is 4.12 dB.

Figures 20 and 21 show the FER performance of the 64QAM 4×4 MIMO systems with SE at 19.2 bits/s/Hz and 20.0 bits/s/Hz, respectively. Figure 20 shows that, compared with the binary LDPC-coded uniform 64QAM no-rotation system with a code rate of 4/5, the optimized 14-degree rotation of the binary LDPC-coded uniform rotated 64QAM system can obtain a 1.70-dB diversity gain, and a further 0.55-dB shaping gain comes from the optimized 14-degree rotation in the binary LDPC-coded PS3 rotated 64QAM system. The total performance gain of the proposed binary LDPC-coded PS3 64QAM MIMO system with SSD is 2.25 dB. Compared with the binary LDPC-coded uniform 64QAM no-rotation system with a code rate of 4/5, the GF(64) LDPC-coded uniform 64QAM no-rotation system with a code rate of 4/5 obtains a 0.75-dB coding gain, and the optimized 14-degree rotation of the GF(64) LDPC-coded uniform rotated 64QAM system gives a 1.42-dB diversity gain. We find a further 0.64-dB shaping gain with the optimized 14-degree rotation of the GF(64) LDPC-coded PS3 rotated 64QAM system. Compared with the GF(64) LDPC-coded uniform 64QAM no-rotation system with a code rate of 4/5, the total performance gain of the optimal GF(64) LDPC-coded PS3 rotated 64QAM system is 2.06 dB.

In Fig. 21, compared with the binary LDPC-coded uniform 64QAM no-rotation system with a code rate of 5/6, we see that the optimized 14-degree rotation of the binary LDPC-coded uniform rotated 64QAM system gives a diversity gain of 2.42 dB, and a further shaping gain of 0.42 dB can be achieved with the optimized 14-degree rotation in the binary LDPC-coded PS4 rotated 64QAM system. Therefore, the total performance gain of the proposed binary LDPC-coded PS4 64QAM MIMO system with SSD is 2.84 dB. Compared with the binary LDPC-coded uniform 64QAM no-rotation system with a code rate of 5/6, the GF(64) LDPC-coded uniform 64QAM no-rotation system with a code rate of 5/6 obtains a 0.70-dB coding gain, and the optimized 14-degree rotation of the GF(64) LDPC-coded uniform rotated 64QAM system produces a 2.14-dB diversity gain. There is a further 0.50-dB shaping gain using the optimized 14-degree rotation of the GF(64) LDPC-coded PS4 rotated 64QAM system. Compared with the GF(64) LDPC-coded uniform 64QAM no-rotation system with a code rate of 5/6, the total performance gain of the optimal GF(64) LDPC-coded PS4 rotated 64QAM system is 2.64 dB.

In fading channels, compared with the conventional uniform QAM system, constellation rotation can obtain a diversity gain and PS produces a shaping gain. Compared with binary LDPC codes, NB LDPC codes achieve a further coding gain. In summary, compared with conventional binary LDPC-coded uniform QAM no-rotation MIMO systems, the proposed NB LDPC-coded PS rotated QAM MIMO system exhibits a coding gain, shaping gain, and diversity gain.

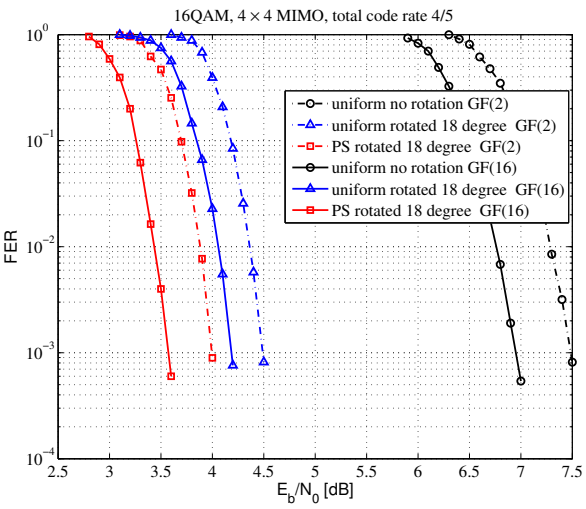

Fig. 18: FER performance of 16QAM 4×4 MIMO systems with SE at 12.8 bits/s/Hz.

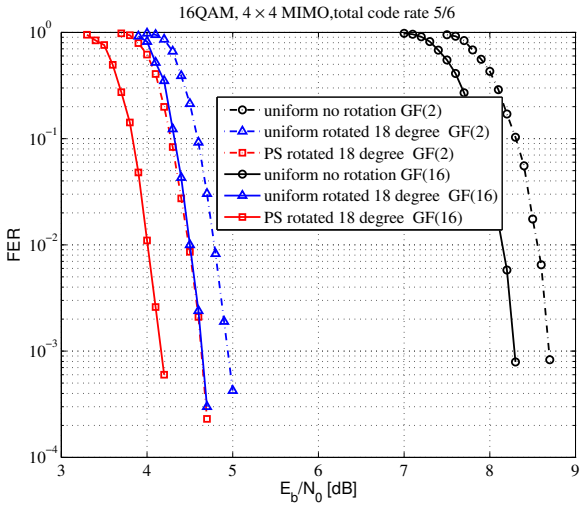

Fig. 19: FER performance of 16QAM 4 × 4 MIMO systems with SE at 13.334 bits/s/Hz.

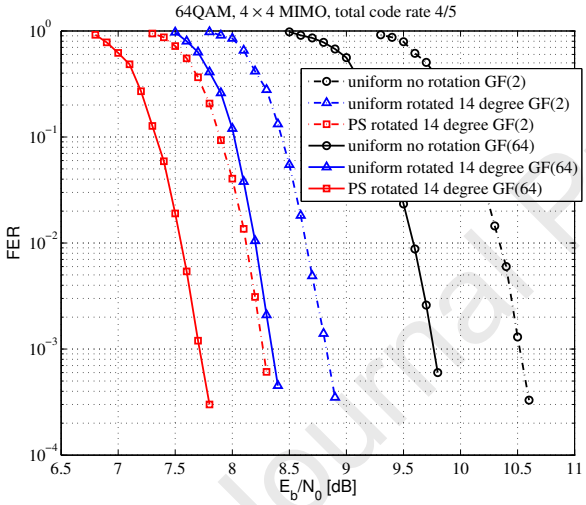

Fig. 20: FER performance of 64QAM 4 × 4 MIMO systems with SE at 19.2 bits/s/Hz.

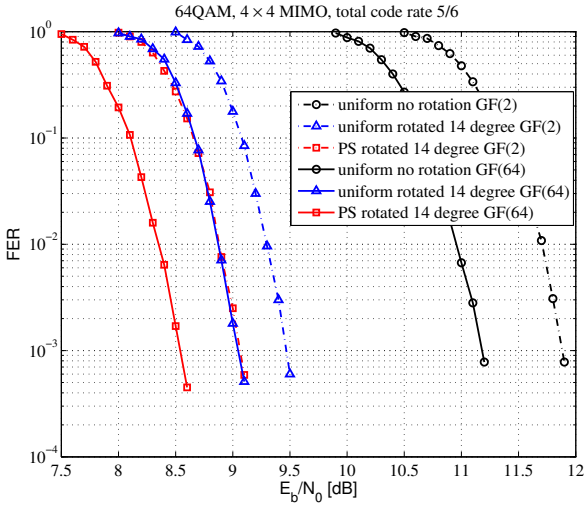

Fig. 21: FER performance of 64QAM 4 × 4 MIMO systems with SE at 20.0 bits/s/Hz.

5. Conclusion

This paper has proposed binary and NB LDPC-coded PS schemes for MIMO systems based on SSD. The NB scheme enables further coding gains to be achieved. Compared with NB LDPC-coded uniform QAM MIMO systems in fast fading channels, the proposed scheme for 2 × 2 and 4 × 4 MIMO systems achieves both a diversity gain and a shaping gain. The theoretical AMI analysis and simulation results show that the proposed NB LDPC-coded PS scheme for MIMO systems based on SSD is reliable and robust, making it suitable for 6G communication systems.

References

[1] S. Han, T. Xie, C.-L. I, Greener physical layer technologies for 6g mobile communications, IEEE Communications Magazine 59 (4) (2021) 68–74.

[2] S. Chen, Y.-C. Liang, S. Sun, S. Kang, W. Cheng, M. Peng, Vision, requirements, and technology trend of 6g: How to tackle the challenges of system coverage, capacity, user data-rate and movement speed, IEEE Wireless Communications 27 (2) (2020) 218–228.

[3] E. Basar, Reconfigurable intelligent surface-based index modulation: A new beyond mimo paradigm for 6g, IEEE Transactions on Communications 68 (5) (2020) 3187–3196.

[4] W. Saad, M. Bennis, M. Chen, A vision of 6g wireless systems: Applications, trends, technologies, and open research problems, IEEE Network 34 (3) (2020) 134–142.

[5] K. David, J. Elmirghani, H. Haas, X.-H. You, Defining 6g: Challenges and opportunities [from the guest editors], IEEE Vehicular Technology Magazine 14 (3) (2019) 14–16.

[6] L. Zheng, D. Tse, Diversity and multiplexing: a fundamental tradeoff in multiple-antenna channels, IEEE Transactions on Information Theory 49 (5) (2003) 1073–1096.

[7] V. Tarokh, N. Seshadri, A. Calderbank, Space-time codes for high data rate wireless communication: performance criterion and code construction, IEEE Transactions on Information Theory 44 (2) (1998) 744–765.

[8] X. Gao, L. Dai, S. Han, C.-L. I, R. W. Heath, Energy-efficient hybrid analog and digital precoding for mmwave mimo systems with large antenna arrays, IEEE Journal on Selected Areas in Communications 34 (4) (2016) 998–1009.

[9] Q. Xie, J. Song, K. Peng, F. Yang, Z. Wang, Coded modulation with signal space diversity, IEEE Transactions on Wireless Communications 10 (2) (2011) 660–669.

[10] H. Lee, A. Paulraj, Mimo systems based on modulation diversity, IEEE Transactions on Communications 58 (12) (2010) 3405–3409.

[11] K. V. Srinivas, R. D. Koilpillai, S. Bhashyam, K. Giridhar, Coordinate interleaved spatial multiplexing with channel state information, IEEE Transactions on Wireless Communications 8 (6) (2009) 2755–2762.

[12] Z. Wu, X. Gao, An efficient mimo scheme with signal space diversity for future mobile communications, EURASIP Journal on Wireless Communications and Networking 2015 (1) (2015) 1–18.

[13] G. Forney, R. Gallager, G. Lang, F. Longstaff, S. Qureshi, Efficient modulation for band-limited channels, IEEE Journal on Selected Areas in Communications 2 (5) (1984) 632–647.

[14] J. Barrueco, J. Montalban, C. Regueiro, M. Vélez, J. L. Ordiales, H.-M. Kim, S.-I. Park, S. Kwon, Constellation design for bit-interleaved coded modulation (bicm) systems in advanced broadcast standards, IEEE Transactions on Broadcasting 63 (4) (2017) 603–614.

[15] A. Calderbank, L. Ozarow, Nonequiprobable signaling on the gaussian channel, IEEE Transactions on Information Theory 36 (4) (1990) 726–740.

[16] G. Böcherer, Labeling non-square qam constellations for one-dimensional bit-metric decoding, IEEE Communications Letters 18 (9) (2014) 1515–1518.

[17] G. Böcherer, F. Steiner, P. Schulte, Bandwidth efficient and rate-matched low-density parity-check coded modulation, IEEE Transactions on Communications 63 (12) (2015) 4651–4665.

[18] F. Steiner, G. Liva, G. Boecherer, Ultra-sparse non-binary ldpc codes for probabilistic amplitude shaping, in: GLOBECOM 2017 - 2017 IEEE Global Communications Conference, 2017, pp. 1–5.

[19] F. Steiner, G. Böcherer, G. Liva, Bit-metric decoding of non-binary ldpc codes with probabilistic amplitude shaping, IEEE Communications Letters 22 (11) (2018) 2210–2213.

[20] P. Schulte, G. Böcherer, Constant composition distribution matching, IEEE Transactions on Information Theory 62 (1) (2016) 430–434.

[21] Z. Wu, W. Kang, A time sharing hybrid probabilistic shaping scheme for nonbinary ldpc codes, IEEE Access 8 (2020) 65488–65497.

[22] M. Pikus, W. Xu, Bit-level probabilistically shaped coded modulation, IEEE Communications Letters 21 (9) (2017) 1929–1932.

[23] W. Kang, A novel nonbinary ldpc-coded time sharing hybrid probabilistic shaping scheme for 128qam, in: 2020 IEEE International Conference on Communications Workshops (ICC Workshops), 2020, pp. 1–6.

[24] T. Fehenberger, D. S. Millar, T. Koike-Akino, K. Kojima, K. Parsons, Parallel-amplitude architecture and subset ranking for fast distribution matching, IEEE Transactions on Communications 68 (4) (2020) 1981–1990.

[25] Y. Yao, K. Xiao, B. Xia, Q. Gu, Design and analysis of rotated-qam based probabilistic shaping scheme for rayleigh fading channels, IEEE Transactions on Wireless Communications 19 (5) (2020) 3047–3063.

[26] T. Richardson, S. Kudekar, Design of low-density parity check codes for 5g new radio, IEEE Communications Magazine 56 (3) (2018) 28–34.

[27] M. Sybis, K. Wesolowski, K. Jayasinghe, V. Venkatasubramanian, V. Vukadinovic, Channel coding for ultra-reliable low-latency communication in 5g systems, in: 2016 IEEE 84th Vehicular Technology Conference (VTC-Fall), 2016, pp. 1–5.

[28] M. Davey, D. MacKay, Low-density parity check codes over gf(q), IEEE Communications Letters 2 (6) (1998) 165–167.

[29] D. Declercq, M. Fossorier, Decoding algorithms for nonbinary ldpc codes over gf(q), IEEE Transactions on Communications 55 (4) (2007) 633–643.

[30] A. Voicila, D. Declercq, F. Verdier, M. Fossorier, P. Urard, Low-complexity decoding for non-binary ldpc codes in high order fields, IEEE Transactions on Communications 58 (5) (2010) 1365–1375.

[31] D. Feng, H. Xu, Q. Zhang, Q. Li, Y. Qu, B. Bai, Nonbinary ldpc-coded modulation system in high-speed mobile communications, IEEE Access 6 (2018) 50994–51001.

[32] Z. Wu, X. Gao, C. Jiang, Nonbinary ldpc-coded spatial multiplexing for rate-2 mimo of dvb-ngh system, IEEE Transactions on Broadcasting 64 (2) (2018) 201–210.

[33] G. Caire, G. Taricco, E. Biglieri, Bit-interleaved coded modulation, IEEE Transactions on Information Theory 44 (3) (1998) 927–946.

[34] F. Kschischang, S. Pasupathy, Optimal nonuniform signaling for gaussian channels, IEEE Transactions on Information Theory 39 (3) (1993) 913–929.

Conflict of interest

The authors declared that they have no conflicts of interest to this work.

We declare that we do not have any commercial or associative interest that represents a conflict of interest in connection with the work submitted.